AIAA JOURNAL
Vol. 44, No. 2, February 2006

# Technical Notes

*TECHNICAL NOTES are short manuscripts describing new developments or important results of a preliminary nature. These Notes should not exceed 2500 words (where a figure or table counts as 200 words). Following informal review by the Editors, they may be published within a few months of the date of receipt. Style requirements are the same as for regular contributions (see inside back cover).*

## Low-Reynolds-Number $k$–$\epsilon$ Model with Elliptic Relaxation Function

M. M. Rahman* and T. Siikonen†
*Helsinki University of Technology, FIN-02015 HUT, Finland*

### Nomenclature

| | | |
|---|---|---|
| $C_f$ | = | friction coefficient |
| $C_\mu$ | = | eddy-viscosity coefficient |
| $E_\epsilon$ | = | source term in dissipation equation |
| $f_\mu$ | = | viscous damping function |
| $h$ | = | channel/step height |
| $k$ | = | turbulent kinetic energy |
| $L$ | = | length scale |
| $P$ | = | turbulent production term |
| $S$ | = | mean strain-rate invariant |
| $T_t$ | = | realizable timescale |
| $t$ | = | time |
| $U_i$ | = | mean velocity components |
| $-\overline{u_i u_j}$ | = | Reynolds stresses |
| $W$ | = | mean vorticity invariant |
| $x_i$ | = | Cartesian coordinates |
| $y^+$ | = | nondimensional normal distance from wall |
| $\epsilon$ | = | turbulent dissipation |
| $\mu$, $\mu_T$ | = | laminar and eddy viscosities |
| $\nu$ | = | molecular kinematic viscosity |
| $\rho$ | = | density |
| $\sigma$ | = | turbulent Prandtl number |

### Introduction

CONSIDERABLE research is devoted to introducing the near-wall effects in the $k$–$\epsilon$ turbulence model.[1–10] However, the modeling of near-wall turbulence with the distance to wall as an explicit parameter renders the model often inappropriate to simulating complex flows involving multiple surfaces, the wall distance of which becomes cumbersome to define. A remedy to this flaw is to develop a model that implicates no explicit wall distance while integrating it toward the solid surface.

In principle, the elliptic relaxation method is an excellent alternative to avoid the use of distance to wall.[3] The wall blocking is governed by an elliptic partial differential equation, that is, a Helmholtz-type equation, and, naturally, nonlocal near-wall effects are taken into account. In Ref. 4 the eddy damping function $f_\mu$ is constructed as a product of empirical and elliptic relaxation functions. The empirical function may augment the potentiality of $f_\mu$ to grow, particularly in near-wall regions, thereby predicting excessive eddy viscosity. In addition, the Kolmogorov length scale in the elliptic relaxation equation contains a large constant that has some precedent in the near-wall region. Nevertheless, the model can be sensitive to this value[3] and may produce unexpected results in comparison with experiments.

The present study appears with recourse to a wall-distance-free low-Reynolds-number $k$–$\epsilon$ turbulence model. The improvement herein springs principally from the modeling of the elliptic relaxation function $f_\mu$ to suppress the excessive eddy viscosity in near-wall regions. The characteristic length scale associated with the elliptic relaxation equation is designed in terms of Kolmogorov and dynamic length scales in conjunction with the invariants of strain-rate and vorticity tensors. Consequently, the large constant-dependent sensitivity of the relaxation function is reduced massively, and the nonlocal effects are explicitly influenced by the mean flow and turbulent variables.The model incorporates an extra source term in the $\epsilon$ transport equation that augments the dissipation level in nonequilibrium flow regions, thus reducing the turbulent kinetic energy and length scale magnitudes to improve prediction of adverse pressure gradient flows involving separation and reattachment. The wall singularity is removed by using a physically appropriate timescale that never falls below the Kolmogorov timescale, representing the timescale realizability enforcement accompanied by the near-wall turbulent phenomena. In addition, the turbulent Prandtl numbers $\sigma_{(k,\epsilon)}$ are adjusted so as to provide substantial turbulent diffusion in the near-wall region. In essence, the model is tensorially invariant, frame-indifferent, and applicable to arbitrary topologies. The performance of the new model is demonstrated through the comparison with experimental and direct numerical simulation (DNS) data of well-documented flows.

### Present Model

The proposed model determines the turbulence kinetic energy $k$ and its dissipation rate $\epsilon$ by the following transport equations:

$$\frac{\partial \rho k}{\partial t} + \frac{\partial \rho U_j k}{\partial x_j} = \frac{\partial}{\partial x_j}\left[\left(\mu + \frac{\mu_T}{\sigma_k}\right)\frac{\partial k}{\partial x_j}\right] + \rho P - \rho\epsilon \tag{1}$$

$$\frac{\partial \rho \epsilon}{\partial t} + \frac{\partial \rho U_j \epsilon}{\partial x_j} = \frac{\partial}{\partial x_j}\left[\left(\mu + \frac{\mu_T}{\sigma_\epsilon}\right)\frac{\partial \epsilon}{\partial x_j}\right] + \frac{(C_{\epsilon 1}\rho P - C_{\epsilon 2}\rho\epsilon + E_\epsilon)}{T_t} \tag{2}$$

where the turbulent production term $P = -\overline{u_i u_j}(\partial U_i/\partial x_j)$. The characteristic/realizable timescale $T_t$ can simply be defined as

$$T_t = \sqrt{k^2/\epsilon^2 + C_T^2(\nu/\epsilon)} = (k/\epsilon)\sqrt{1 + C_T^2 \big/ Re_T}$$

$$Re_T = k^2/\nu\epsilon \tag{3}$$

where $\nu$ denotes the kinematic viscosity and $Re_T$ is the turbulence Reynolds number. The turbulence timescale is $k/\epsilon$ at large $Re_T$

Received 16 December 2004; revision received 6 October 2005; accepted for publication 6 October 2005. 

*Research Scientist, Department of Mechanical Engineering, Laboratory of Applied Thermodynamics, Sähkömiehentie 4.

†Professor, Department of Mechanical Engineering, Laboratory of Applied Thermodynamics, Sähkömiehentie 4.

but approaches the Kolmogorov limit $C_T\sqrt{(\nu/\epsilon)}$ for $Re_T \ll 1$. It prevents the singularity in the dissipation equation down to the wall. The associated empirical constants are: $C_T = \sqrt{2}$, $C_{\epsilon 1} = 1.44$, and $C_{\epsilon 2} = 1.83$.

Because the viscous dissipation presumably dominates near the wall, the eddy viscosity is evaluated from

$$\mu_T = C_\mu f_\mu \rho k T_t, \qquad f_\mu = \sqrt{C_\mu}\Big/(C_T + Re_T) + f_w^2 \tag{4}$$

where $C_\mu = 0.09$ and the dynamic timescale $k/\epsilon$ is replaced by $T_t$, a distinct turbulence timescale. To eradicate the complexity/empiricism in defining the wall distance with multiple surfaces, a Helmholtz-type elliptic relaxation equation for $f_w$ is introduced. It represents a general ellipticity, pertaining to $f_w$ without the knowledge of the wall distance,

$$-L^2\nabla^2 f_w + f_w = 1 \tag{5}$$

where $L$ is the characteristic length scale. To avoid the singularity close to the wall, the Kolmogorov length scale $(\nu^3/\epsilon)^{1/4}$ is added to the dynamic length scale $k^{3/2}/\epsilon$. After some manipulations, a compatibility relation is deduced as

$$L^2 = \nu\zeta\left[C_\mu Re_T(k/\epsilon) + 4\xi^2\sqrt{\nu/\epsilon}\right] \tag{6}$$

where $\zeta = C_T\sqrt{(\nu/\epsilon)}\eta$ and $\xi = T_t\eta$. The parameter $\eta = \max(S, W)$, containing the invariants $S = \sqrt{(2S_{ij}S_{ij})}$ and $W = \sqrt{(2W_{ij}W_{ij})}$. The mean strain-rate and mean vorticity tensors $S_{ij}$ and $W_{ij}$ are defined as

$$S_{ij} = \frac{1}{2}\left(\frac{\partial U_i}{\partial x_j} + \frac{\partial U_j}{\partial x_i}\right), \qquad W_{ij} = \frac{1}{2}\left(\frac{\partial U_i}{\partial x_j} - \frac{\partial U_j}{\partial x_i}\right) \tag{7}$$

The rationale with the present approach is that the wall proximity effect is modeled naturally in conjunction with the elliptic relaxation function $f_\mu$. The virtue of Eq. (5) is that, unlike the Poisson equation, it requires no special numerical treatment. It can be solved in parallel with the $k$–$\epsilon$ equations having an initial guess $0 \le f_w \le 1$ everywhere except on wall boundaries where $f_w = 0$.

Obviously, $f_\mu$ is valid in the whole flowfield, including the viscous sublayer and the logarithmic layer. As evinced by Fig. 1 in comparison with the DNS data[11] for a fully developed turbulent channel flow, the adopted form of $f_\mu$ reproduces correctly the asymptotic limit involving the distinct effects of low Reynolds-number and wall proximity. In Fig. 1, the So–Sakar–Gerodimos–Zhang (SSGZ)[5] and modified Chien (MCH) (see Ref. 8) models are represented. The proposed function $f_\mu = 1$ is remote from the wall to ensure that

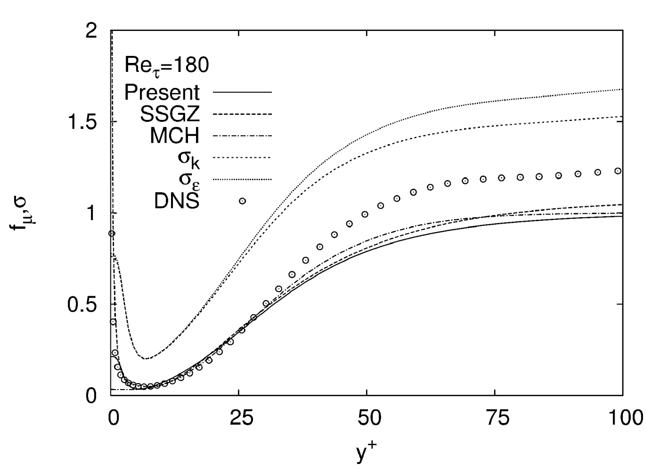


**Fig. 1 Variations of damping functions with wall distance in channel flow.**

the model is compatible with the standard $k$–$\epsilon$ turbulence model. To this end, note that, in Eq. (6), the second term in parenthesis is needed to obtain adequate wall blocking. Otherwise, the predicted turbulent viscosity could be too large near the wall. Furthermore, the empirical function associated with $f_\mu$ (unlike the commonly adopted practice) in Eq. (4) reduces the potentiality of $f_\mu$ to grow, particularly in near-wall regions as represented by Fig. 1, thereby facilitating avoidance of excessive eddy viscosity.

The budgets of $k$ and $\epsilon$ from the DNS data prove that the role of turbulent diffusion in the near-wall region is substantial. Accordingly, the Prandtl numbers $\sigma_k$ and $\sigma_\epsilon$ are modeled, rather than being assigned constant values:

$$\sigma_\epsilon = C_T^2\Big/(1+\xi) + f_\mu^{\frac{3}{4}}, \qquad \sigma_k = \sigma_\epsilon\Big/\left(1 - C_\mu f_\mu^{\frac{3}{4}}\right) \tag{8}$$

The distribution of $\sigma$ is shown in Fig. 1. The model coefficients $\sigma_k$ and $\sigma_\epsilon$ are developed such that sufficient diffusion is obtained in the vicinity of the wall and in the core region of the flow $\sigma_k/\sigma_\epsilon > 1$ to eliminate the common drawback where the turbulent diffusion of $k$ overwhelms the diffusion of $\epsilon$ with $\sigma_k < \sigma_\epsilon$ (Ref. 2).

The extra source term $E_\epsilon$ in Eq. (2) is constructed from the cross-diffusion model[10] as

$$E_\epsilon = C_\epsilon \frac{\mu_T}{T_t}\max\left[\frac{\partial(k/\epsilon)}{\partial x_j}\frac{\partial k}{\partial x_j}, 0\right], \qquad C_\epsilon = \sqrt{C_{\epsilon 1}^2 + C_{\epsilon 2}^2} \tag{9}$$

The source term $E_\epsilon$ is characteristically beneficial in the vicinity of adverse pressure gradient flows accompanied by flow separation and reattachment. Obviously, the quantity $E_\epsilon$ stimulates the energy dissipation in nonequilibrium flows, thereby reducing the departure of the turbulent length scale from its local equilibrium value and enabling improved predictions.

## Computations

To ascertain the efficacy of the proposed model, a few applications to two-dimensional turbulent flows consisting of a fully developed channel flow, a backward-facing step flow, and an asymmetric plane diffuser flow are considered. For comparison purposes, calculations from the SSGZ and MCH models are included. Note that both the SSGZ and MCH models contain the wall distance. A cell-centered finite volume scheme combined with an artificial compressibility approach[12] is employed to solve the flow equations.

## Channel Flow

The computation is carried out for fully developed turbulent channel flows at $Re_\tau = 180$ and 395, for which turbulence quantities are attainable from the DNS data.[11] Calculations are conducted in the half-width of the channel, imposing cyclic boundary conditions except for the pressure. The length of the computational domain is $32\delta$, where $\delta$ is the channel half-width. A $96 \times 64$ nonuniform grid refinement is considered based on the grid-independence test. To ensure the resolution of viscous sublayer, the first grid node near the wall is placed at $y^+ \approx 0.3$. Comparisons are made by plotting the results in wall units. The results shown in Figs. 2 and 3 indicate that the present model predictions are in broad accord with other models and DNS data.

## Backward-Facing Step Flow

To validate the performance in complex separated and reattaching turbulent flows, the present model is applied to the flow over a backward-facing step. The computation is conducted corresponding to the experimental case with zero deflection of the wall opposite to the step, as investigated by Driver and Seegmiller.[13] The ratio between the channel height and the step height $h$ is 9, and the step height Reynolds number is $Re = 3.75 \times 10^4$. At the channel inlet, the Reynolds number based on the momentum thickness is $Re_\theta = 5 \times 10^3$. A $128 \times 128$ nonuniform grid is used for the computations, and the maximum height of the first near-wall grid node is at $y^+ < 1.5$. The inlet profiles for all dependent variables are generated by solving the models at the appropriate momentum thickness Reynolds number. The distance $x/h$ shown hereafter is measured exactly from the step corner.

Computed and experimental friction coefficients $C_f$ along the step side wall are shown in Fig. 4. As is observed, all models are in good agreement with the data. However, the SSGZ model exhibits a nonphysical trend in the $C_f$ profile near the corner at the base of the step. This is probably due to the improper behavior of the viscous damping functions employed. The recirculation lengths predicted by the present, SSGZ, and MCH models are 6.4$h$, 6.0$h$, and 6.8$h$, respectively. The experimental value of the reattachment length is $6.26 \pm 0.1$, making a fairly good correspondence with all models. Comparisons are extended to the distributions of Reynolds shear stress and the corresponding turbulent kinetic energy at different $x/h$ locations behind the step corner, as shown in Figs. 5 and 6. A closer inspection of the distribution indicates that all model predictions are in a broad agreement with the experimental data.

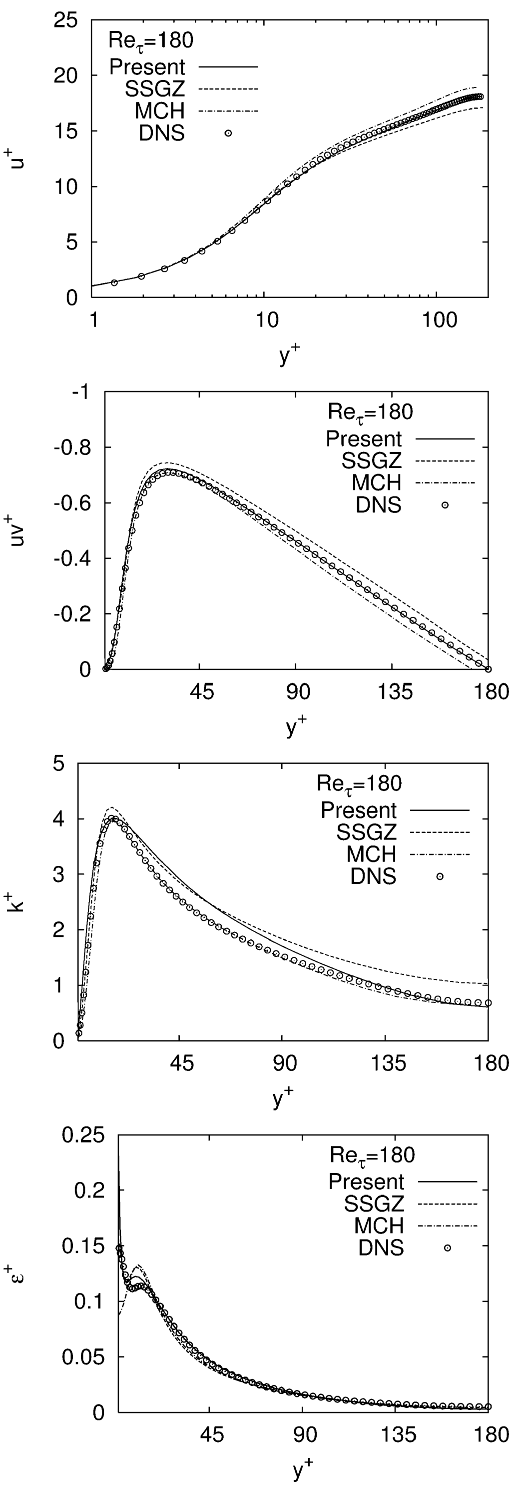


**Fig. 2 Channel flow predictions compared with DNS at $Re_\tau = 180$.**

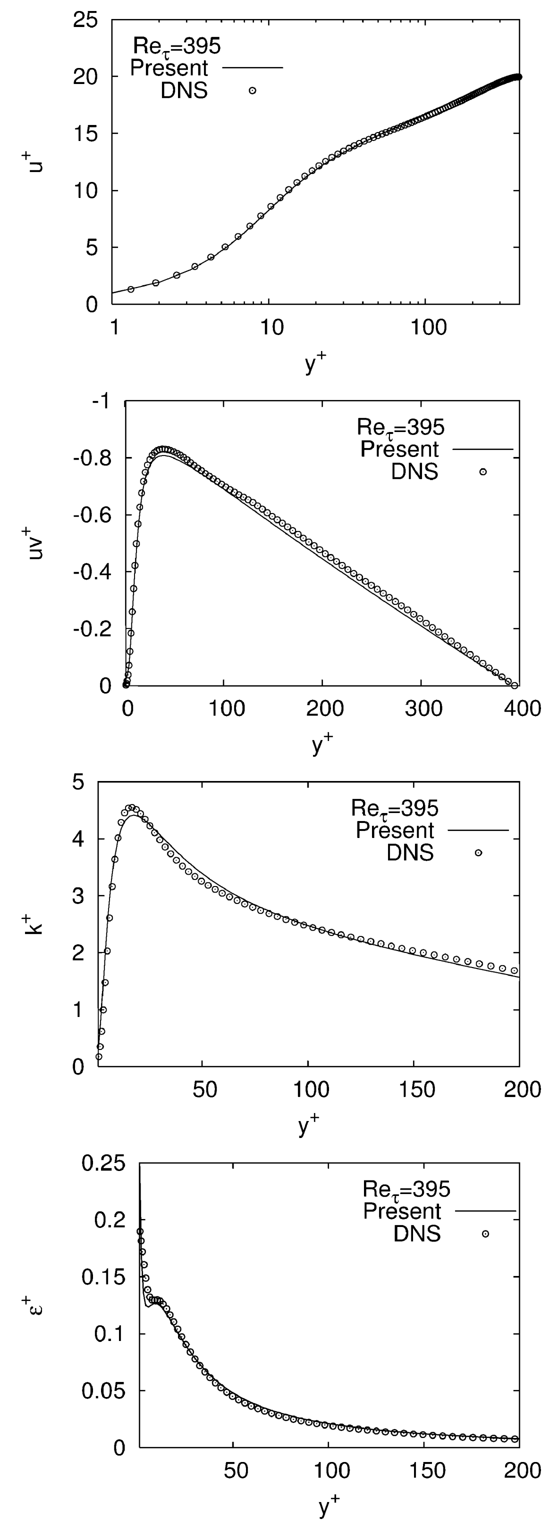


**Fig. 3 Channel flow predictions compared with DNS at $Re_\tau = 395$.**

## Asymmetric Plane Diffuser Flow

To further evaluate the performance, the model is applied to simulate the flow in a plane asymmetric diffuser with an opening angle of 10 deg, for which measurements are available.[14] The expansion ratio of 4.7 is sufficient to produce a separation bubble on the deflected wall. Hence, the configuration provides a test case for smooth, adverse pressure-driven separation. The entrance to the diffuser consists of a plane channel to invoke fully developed flow with $Re = 2 \times 10^4$ based on the centerline velocity and the channel height.

Computations involving a $120 \times 72$ nonuniform grid resolution are considered to be accurate to describe the flow characteristics. The length of the computational domain is $76h$, where $h$ is the inlet channel height. The thickness of the first cell remains below one in the $y^+$ unit on both the deflected and flat walls. Figure 7

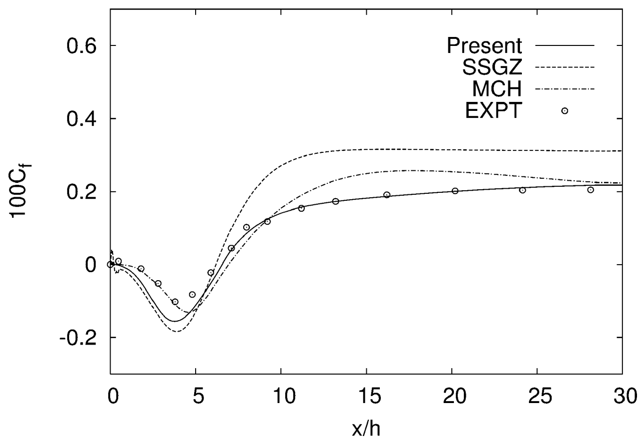


**Fig. 4 Skin-friction coefficient along step-side bottom wall.**

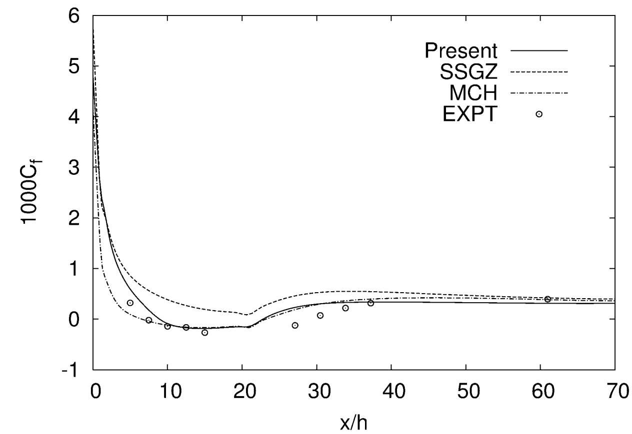


**Fig. 7 Skin-friction coefficient of diffuser flow along deflected bottom wall.**

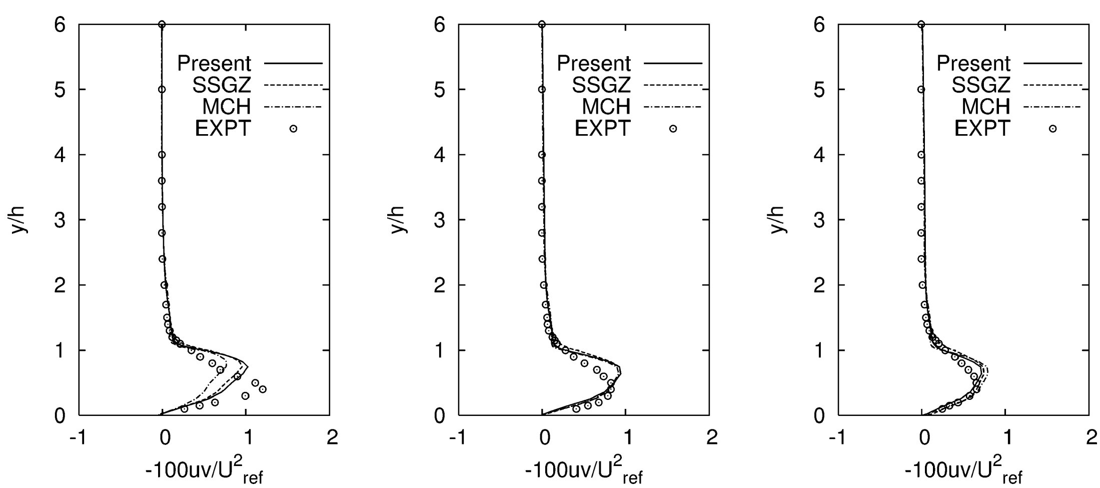


**a) $x/h = 4.0$** **b) $x/h = 6.0$** **c) $x/h = 8.0$**

**Fig. 5 Shear stress profiles at selected locations for step flow.**

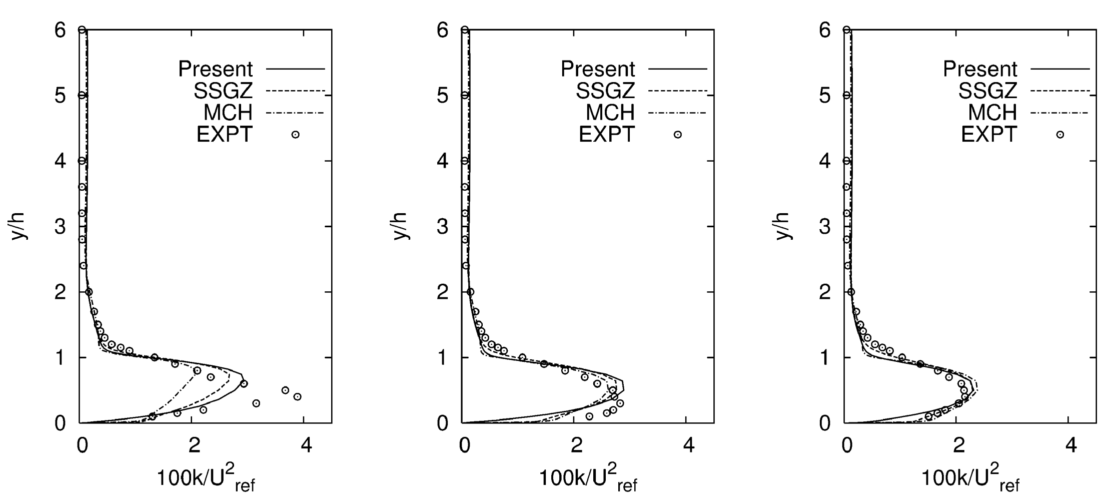


**a) $x/h = 4.0$** **b) $x/h = 6.0$** **c) $x/h = 8.0$**

**Fig. 6 Kinetic energy profiles at selected locations for step flow.**

shows the predicted skin-friction coefficients $C_f$. The performance of both the present and MCH models evinces an encouraging qualitative agreement with measurements. Apparently, the ambiguous prediction regarding the SSGZ model demands a higher value for the proposed correction in the $\epsilon$ equation to render the model results compatible with the experiment.

## Conclusions

The proposed turbulent model resolves the near-wall and low-Reynolds-number effects using the $f_\mu$ elliptic relaxation equation. It is wall-distance free, tensorially invariant, and frame indifferent and, hence, applicable to arbitrary topology. The anisotropic production in the dissipation equation is accounted for substantially by adding a secondary source term. The model is capable of evaluating the flow cases entangling separation and reattachment. Contrasting the predicted results with experiments demonstrates that the present model replicates fairly well the influence of wall proximity and retrieves the aspects of other models with the wall distance in the damping functions.

## References


[1]Patel, V. C., Rodi, W., and Scheuerer, G., "Turbulence Models for Near-Wall and Low-Reynolds-Number Flow: A Review," *AIAA Journal*, Vol. 23, No. 9, 1985, pp. 1308–1319.

[2]Nagano, T., and Tagawa, M., "An Improved $k$–$\epsilon$ Model for Boundary Layer Flows," *Journal of Fluids Engineering*, Vol. 112, June 1990, pp. 33–39.

[3]Durbin, P. A., "Near-Wall Turbulence Closure Modeling Without Damping Function," *Theoretical and Computational Fluid Dynamics*, Vol. 3, No. 1, 1991, pp. 1–13.

[4]Park, T. S., and Sung, H. J., "A New Low-Reynolds Number $k$–$\epsilon$–$f_\mu$ Model for Predictions Involving Multiple Surfaces," *Fluid Dynamics Research*, Vol. 20, No. 1–6, 1997, pp. 97–113.

[5]So, R. M. C., Sarkar, A., Gerodimos, G., and Zhang, J., "A Dissipation Rate Equation for Low-Reynolds Number and Near-Wall Turbulence," *Theoretical and Computational Fluid Dynamics*, Vol. 9, No. 1, 1997, pp. 47–63.

[6]Sarkar, A., and So, R. M. C., "A Critical Evaluation of Near-Wall Two-Equation Models Against Direct Numerical Simulation Data," *International Journal of Heat and Fluid Flow*, Vol. 18, No. 2, 1997, pp. 197–208.

[7]Hwang, C. B., and Lin, C. A., "Improved Low-Reynolds-Number $k$–$\tilde{\epsilon}$ Model Based on Direct Numerical Simulation Data," *AIAA Journal*, Vol. 36, No. 1, 1998, pp. 38–43.

[8]Rahman, M. M., and Siikonen, T., "Improved Low-Reynolds-Number $k$–$\tilde{\epsilon}$ Model," *AIAA Journal*, Vol. 38, No. 7, 2000, pp. 1298–1300.

[9]Rahman, M. M., and Siikonen, T., "Low-Reynolds-Number $k$–$\tilde{\epsilon}$ Model with Enhanced Near-Wall Dissipation," *AIAA Journal*, Vol. 40, No. 7, 2002, pp. 1462–1464.

[10]Rahman, M. M., and Siikonen, T., "Near-Wall Turbulence Modelling with Enhanced Dissipation," *International Journal for Numerical Methods in Fluids*, Vol. 42, No. 9, 2003, pp. 979–997.

[11]Mansour, N. N., Kim, J., and Moin, P., "Reynolds-Stress and Dissipation-Rate Budgets in a Turbulent Channel Flow," *Journal of Fluid Mechanics*, Vol. 194, 1988, pp. 15–44.

[12]Rahman, M. M., Rautaheimo, P., and Siikonen, T., "Numerical Study of Turbulent Heat Transfer from a Confined Impinging Jet Using a Pseudo-Compressibility Method," *2nd International Symposium on Turbulence, Heat and Mass Transfer*, Delft Univ. Press, Delft, The Netherlands, 1997, pp. 511–520.

[13]Driver, D. M., and Seegmiller, H. L., "Features of a Reattaching Turbulent Shear Layer in Divergent Channel Flow," *AIAA Journal*, Vol. 23, No. 2, 1988, pp. 163–171.

[14]Buice, C., and Eaton, J. K., "Experimental Investigation of Flow Through an Asymmetric Plane Diffuser," Dept. of Mechanical Engineering, Thermosciences Div., Rept. TSD-107, Stanford Univ., Stanford, CA, 1997.


S. Mahalingam
*Associate Editor*